European Journal of Molecular & Clinical Medicine

ISSN 2515-8260 Volume 09, Issue 02, 2022

Ultrasonography and CT evaluation of neck masses

[1]Dr. Neha Goel, [2]Dr. Bindu Agrawal, [3]Dr. Amritanshu, [4]Dr. Gaurav Gupta, [5]Dr. Kumar Ritwik, [6]Dr. Venkteshwara

[1,5,6]Junior Resident, Muzaffarnagar Medical College, Muzaffarnagar, Uttar Pradesh, India
[2]Professor and HOD, Muzaffarnagar Medical College, Muzaffarnagar, Uttar Pradesh, India
[3]Senior Resident, Muzaffarnagar Medical College, Muzaffarnagar, Uttar Pradesh, India
[4]Assistant Professor, Muzaffarnagar Medical College, Muzaffarnagar, Uttar Pradesh, India

Corresponding Author:
Dr. Gaurav Gupta (683gaurav@gmail.com)

Abstract

Background: A palpable neck mass is a commonly encountered clinical problem. They vary in etiology, pathology, and prognosis due to the complicated anatomy and physiology. This study was done to detect the effectiveness of high-resolution ultrasonography and computed tomography imaging in detecting neck masses.

Aim and Objectives:

1. To assess the utility of High-Resolution Ultrasonography and Computed Tomography imaging in the evaluation of neck masses.
2. To study mass lesions under the following headings- Location, Size and extent of the mass, relation to surrounding structures, internal mass characteristics that are benign or malignant.

Material and methods: The hospital-based prospective observational study was conducted in the Department of Radio diagnosis & Imaging, Muzaffarnagar Medical College, U.P. for eighteen months, with twelve months for data collection and six months for data analysis. A total of 40 patients of varied age groups presenting with a clinically palpable neck mass who underwent both USG and CT were studied.

Results: The maximum number of patients was 41-50 years old (28%), followed by 21-30 years (12.5%). Of the total cases (40), non-nodal masses were 22 (55%), and nodal masses were 18 (45%). The most common pathology in the present study was lymph nodal mass of aerodigestive malignancies, noted in 13 cases (32.5%), and followed by thyroid mass, noted in 12 cases (30%).

Conclusion: High-resolution sonography is valuable modality for the diagnostic evaluation of neck masses in every age group. It is a simple, non-invasive, and inexpensive diagnostic tool. It provides accurate and reproducible results. It can be used as a first-line modality for evaluating cervical soft tissue masses in many clinical conditions, especially in young and pediatric populations. CT ensures accurate anatomical localization and lesion characterization in benign lesions. It is helpful in staging malignant tumours and provides essential information about the tumour extent that directly affects the surgical approach necessary for curative resection.

Keywords: High-resolution ultrasound, computed tomography, neck masses

ISSN 2515-8260 Volume 09, Issue 02, 2022

Introduction

The presence of a palpable neck lump is a common clinical concern. Because of their intricate anatomy and physiology, they have a wide range of aetiology, pathophysiology, and prognosis [1]. Before beginning any treatment, imaging is increasingly used to establish the clinical diagnosis and characterize the anatomical extent of involvement. Despite the overlapping appearances, the lesions can typically be distinguished based on specific imaging findings and pertinent clinical information [2].

For neck tumours, high-resolution ultrasonography is an excellent first imaging study. It is widely available, reasonably priced, good spatial and contrast resolution and does not use ionising radiation. Ultrasound also provides accurate, real-time guidance for FNAC or core biopsies.

CT imaging efficiently aids in diagnosis of a variety of clinical illnesses, such as congenital abnormalities, infections, inflammations, neoplasms, and traumatic events. It also provides information on regional lymph nodes and vascular structure [3], as well as assisting in the evaluation of extension to adjacent structures. CT scans are very helpful in the staging and preoperative evaluation of head and neck cancers. The use of helical CT has resulted in improved resolution as well as a significant reduction in scan acquisition and display time. This technique contributes to greater lesion conspicuity by improving temporal resolution into arterial and venous phases, volume capture of data for easier retrospective reconstruction, isotropic viewing, and endless reformations. Spiral CT is today considered the "gold standard" for neck imaging [4].

CT improves soft tissue detail and air space demarcation significantly. Contrast-enhanced images can be used to analyze the vascularity of the lesion and its relationship to vascular structures5. CT's ability to offer tissue attenuation values is also useful in determining the type of lesion. It can reveal the entire neck lesion as well as an extension of large neck masses. Despite the fact that CT scanning exposes patients to radiation, the increased visualization of neck structures outweighs the risk (excellent benefit to risk ratio) [14].

The goal of this research was to see how successful high-resolution ultrasonography and computed tomography imaging are at detecting neck masses.

Aim and Objectives

1. To evaluate the role of USG and CT imaging in evaluation of neck masses.
2. To study mass lesions under following headings.

- Location.
- Size and extent of the mass.
- Relation to surrounding structures.
- Internal characteristics of the mass.
- Benign or malignant.

Material and Methods

The hospital-based prospective observational study took place in Department of Radio diagnosis & Imaging at Muzaffarnagar Medical College in Uttar Pradesh for eighteen months, with twelve months for data collection and six months for data analysis. A total of 40 patients were investigated who presented with a clinically palpable neck mass and underwent both USG and CT.

ISSN 2515-8260 Volume 09, Issue 02, 2022

Inclusion criteria

Patients with a clinically palpable neck mass underwent Ultrasonography and CT scan, and the results were compared to the final histopathological report.

Exclusion criteria

- Post-operative patients.
- Patients with contraindications to intravenous administration to contrast medium.
- Pregnant females

Procedure

High resolution ultrasonography and color Doppler Imaging.

Patient preparation: Informed written consent was taken prior to the procedure.

Machine used: Samsung H6O and Alpinion Ecube 8.

Procedure

The sonographic examination of the neck was performed in a supine position, with the patient's neck hyper-extended and a pad or pillow under the shoulders to give optimal neck exposure. The mass was examined in both longitudinal and transverse planes to determine its size, form, consistency, and echogenicity. It was also examined for its internal architecture, septae, calcification, and necrosis. To maximise doppler sensitivity, the scanning was done at a slow frame rate with a low pulse repetition frequency, a narrow gate, a low wall filter setting, and a high doppler gain setting.

CT (Computerized Tomography)

Prior renal function tests were performed on the patient. Prior to the scan, the patients were kept on an empty stomach for 4-6 hours. Written informed consent was obtained.
Position-Supine with the neck slightly extended so that the hard palate is roughly perpendicular to the table surface. When possible, the scanning was performed with the patient breathing quietly and swallowing stopped. Siemens Somatom Scope 16 slice machine was utilised.
Procedure: Non-enhanced and contrast-enhanced scans were conducted in order (60 ml contrast administered at 2-3 ml/sec with bolus tracking).

Scanning parameters

- Base of the skull to the lung apices
- 5-mm collimation.
- Matrix: 512 x 512
- kV and mAs: 120 kVp and 100-300 mAs

ISSN 2515-8260 Volume 09, Issue 02, 2022

- Slice thickness: 2.5 mm
- Multiplanar reconstruction using 0.75 mm axial sections with bone and soft tissue algorithm.

The cytopathological or histopathological examination reports of all patients were collected from the pathology department and were used as a gold standard to compare with USG diagnosis and Multidetector CT diagnosis.

Results

Table 1: Gender distribution among the study subjects

Gender	N	%
Male	26	65
Female	14	35
Total	40	100

The current study was conducted at the Department of Radio-diagnosis and Imaging on patients with neck masses who presented to both the OPD and the IPD. There were 65 percent males and 35 percent females among the 40 participants (Table 1).

Table 2: Age distribution among the study subjects

Age Group (in years)	N	%
1-10	3	7.5
11-20	4	10
21-30	5	12.5
31-40	4	10
41-50	11	27.5
51-60	10	25
61-70	2	5
>70	1	2.5
Total	40	100

The patients in this study ranged in age from one to eighty years old. The age range 41-50 years had the highest number of patients (27.5 percent). 7.5 percent of the participants were over the age of 60. Only 7.5 percent of the participants were between the ages of 1 and 10. (Table 2).

Table 3: Lymph nodal masses vs. Non lymph nodal masses

Final diagnosis	N	%
Nodal masses	18	45
Non Nodal Masses	22	55

Nodal and non-nodal masses constituted 45% and 55% of the total number of cases respectively (Table 3).

Table 4: Benign and malignant lesions according to HPE

Final diagnosis (n=40)	Non nodal masses (n= 22)	Nodal masses (n=18)	Total
Benign lesions	18	5	23
Malignant lesions	4	13	17
Total	22	18	40

13 of the 18 lymph nodal tumours were malignant, while the other five were benign. Four of the 22 non-nodal tumours were malignant, whereas the other 18 were benign. There were 23 cases with benign pathology and 17 cases with malignant pathology in total (Table 4).

Table 5: Multidetector CT diagnosis vs HPE diagnosis (N=40)

CT Findings	No. of cases diagnosed on CT	Total number of cases of the same pathology according to HPE	CT			
			TP	FP	FN	TN
Thyroiditis	0	1	0	0	1	0
Multinodular goiter	4	8	4	0	4	0
Aerodigestive malignancy with metastatic nodes	13	13	13	0	0	0
Pleomorphic adenoma of parotid	1	1	1	0	0	0
Tubercular adenopathy	3	3	3	0	0	0
Retrophryngeal abscess with lymph nodes	1	1	1	0	0	0
Tonsillar abscess with lymph nodes	1	1	1	0	0	0
Carcinoma thyroid	1	3	1	0	2	0
Sialadenitis with sialolithiasis of submandibular gland	1	1	1	0	0	0
Warthin's tumor	0	1	0	0	1	0
Parotid abscess	1	1	1	0	0	0
Carcinoma of parotid	1	1	1	0	0	0
Second branchial cyst	1	1	1	0	0	0
Lipoma	2	2	2	0	0	0
Lymphangioma	1	1	1	0	0	0
Fibromatosis Colli	1	1	1	0	0	0

TP: true positive, FP; False Positive, FN: False Negative TN: True Negative
CT made a correct diagnosis in 32 out of 40 cases (Table 5).

Table 6: USG diagnosis vs HPE diagnosis (N=40)

HPE Findings	No. of cases diagnosed on USG	Total number of cases of the same pathology according to HPE	USG			
			TP	FP	FN	TN
Multinodular goiter	8	8	8	0	0	0
Malignant nodes	8	13	8	0	5	0
Pleomorphic adenoma of parotid	1	1	1	0	0	0
Thyroiditis	1	1	1	0	0	0
Sialadenitis with sialolithiasis of submandibular gland	1	1	1	0	0	0
Warthin's tumor of parotid	1	1	1	0	0	0
Tubercular adenopathy	3	3	3	0	0	0
Parotid abscess	1	1	1	0	0	0
Inflammatory nodes	1	2	1	0	1	0
Carcinoma thyroid	3	3	3	0	0	0
Carcinoma of parotid	1	1	1	0	0	0
Second branchial cyst	1	1	1	0	0	0
Lipoma	2	2	2	0	0	0
Lymphangioma	1	1	1	0	0	0
FibromatosisColli	1	1	1	0	0	0

TP: true positive, FP; False Positive, FN: False Negative TN: True Negative
Ultrasound made a correct diagnosis in 34 out of 40 cases (table 6).

Discussion

40 patients with clinically palpable neck masses were evaluated using Ultrasonography and CECT and the masses were characterized based on location, morphological characteristics and enhancement pattern. The extent was outlined in terms of involvement of adjacent structures, vessels and lymphadenopathy. Cytological, histopathological and/or surgical

details were noted to achieve the final diagnosis.

The overall male to female ratio in our study was 1.8:1, showing that males outnumbered females. The age groups 41-50 and 51-60 years old had the most patients. This was in line with research by Charan *et al.* [7], who found that the majority of patients were in the 40-60-year age category, accounting for 29% of cases, with a male preponderance of 2.1:1. The findings also matched those of Chandra Dev Sahu *et al.* [15], who found that the majority of patients were between the ages of 50 and 60.

In our investigation, nodal masses were found in 18 of the 40 instances, accounting for 45 percent of the total. Metastatic adenopathy from aerodigestive tract malignancies was the most common cause, followed by tubercular lymphadenopathy. Thirteen of the 18 nodal tumours were revealed to be malignant, whereas five were benign. This was supported by a research by Ajay K Gautam *et al.* [11], who found that nodal masses accounted for 45 percent of all cases (18 out of 40), with aero digestive cancers being the most common cause of nodal mass of the neck. This was also supported by research by Charan *et al.* [7], which found that 45 percent of metastatic nodes from known malignancies.

In our study, 13 cases of metastatic adenopathy owing to aerodigestive malignancies were discovered, all of which were histopathologically confirmed to be squamous cell carcinoma of varying grades. All of the malignant tumours in the larynx and pharynx were squamous cell carcinomas, which matches the findings of Becker *et al.* [8], who found that over 90% of lesions were squamous cell carcinomas.

Criteria for metastatic adenopathy

1. Lymph node size was > 1cm in short axis diameter.
2. Intranodal necrosis.
3. Loss of central hilar fat.
4. Increased internal vascularity.
5. Heterogeneous enhancement pattern on CECT.
6. Invasion into surrounding structures.

There were three incidences of tubercular adenopathy found. The tubercular lymph nodes appeared as a conglomerate/matted nodal mass on USG and CT, with rim enhancement (on CT) and fascial plane preservation around them. They reveal no internal vascularity and a loss of central hilar fat. These findings were consistent with those reported by Ajay K Gautam *et al.* [11] and Vaid S *et al.* [9].

Two cases of abscess were discovered in our study, one in the perivertebral space and the other in the tonsillar fossa, in patients who presented with painful swelling, fever, leucocytosis and neutrophilia. On CT, the abscess had entire rim enhancement. In their investigation, Freling N, Roele E, *et al.* [12] concluded that in such circumstances, appropriate clinical assessment is possible; imaging is simply required to characterize the extent of the infective process.

Non-nodal masses accounted for 22 of the 40 instances in our study (55 percent of total cases). Ajay K Goutam *et al.* [11] found that 62 percent of cases (31 out of 50) were non nodal masses, and Chandra Dev Sahu *et al.* [15] found that 73 percent of cases (44 out of 60) were non nodal masses. Thyroid masses were discovered to be the most common cause of non-nodal masses in our investigation, accounting for 55% (n=12) of all non-nodal masses.

In our research, 12 incidences of thyroid cancer were discovered. Thyroid tumours were determined to be malignant in 25% (N=3) of cases and benign in 75% (N=9) of cases. Two cases of papillary carcinoma of the thyroid and one case of medullary carcinoma of the thyroid were among the malignant lesions. The findings matched those of Ajay K Gautam *et al.* [11], who found that out of ten cases of thyroid origin, eight were multinodular goitre and

ISSN 2515-8260 Volume 09, Issue 02, 2022

two were malignant.

Papillary cancer was heteroechoic on USG, with microcalcifications and strong internal vascularity, hereas medullary carcinoma seemed similar but was more aggressive. Papillary cancer did not have any metastatic nodes, whereas medullary carcinoma did. They c ould also be detected on CT as irregular heterogeneously enhancing tumours with loss of fat planes and some metastatic lymph nodes. The USG correctly predicted all cases of multinodular goitre, but the CT correctly predicted just four cases. According to our research, ultrasonography is a better diagnostic technique for predicting multinodular goiter/colloid nodule than CT. There were a total of 5 instances with origins in the salivary glands.

A single malignant lesion (mucoepidermoid carcinoma of the parotid) was found among the salivary gland lesions, accounting for 20% of the total cases, with the other 80% of the lesions being benign. Harriet C. Thoeny *et al.* [10] found similar results in their investigation, finding that 91 percent of the lesions were benign (44 out of 50 cases).

Lipoma was found in three cases, two in the sternocleidomastoid muscle and one in the subcutaneous plane of the submandibular region. They had well-defined margins and uniform attenuation values of -110 to -20 HU on CT scans, with little contrast uptake. Fat cells were discovered with FNAC. According to Ajay K Gautam *et al.* [11] and Charan *et al.* [7], this was the case. In our investigation, lymphangioma (1 case), branchial cyst (1 case) and fibromatosis colli were all classified as masses of developmental origin (1 case).

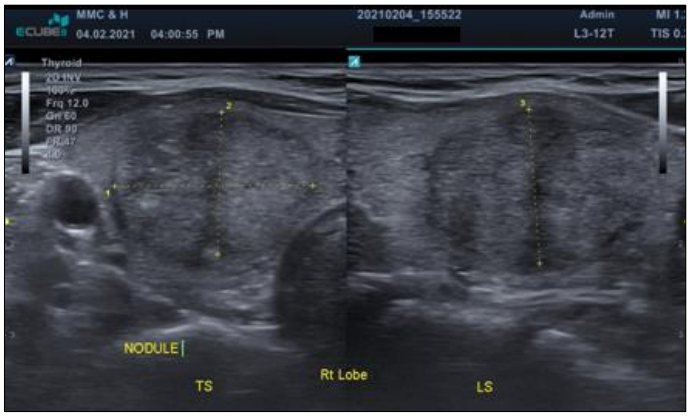

Image 1: Multinodular goiter. 46 years old male with swelling in midline of neck. On USG, B/L lobes of thyroid gland had multiple heterogeneous nodules with hypoechoic halo and peripheral vascularity. The image shows a well-defined heteroechoic nodule in right lobe of thyroid with hypoechoic halo.

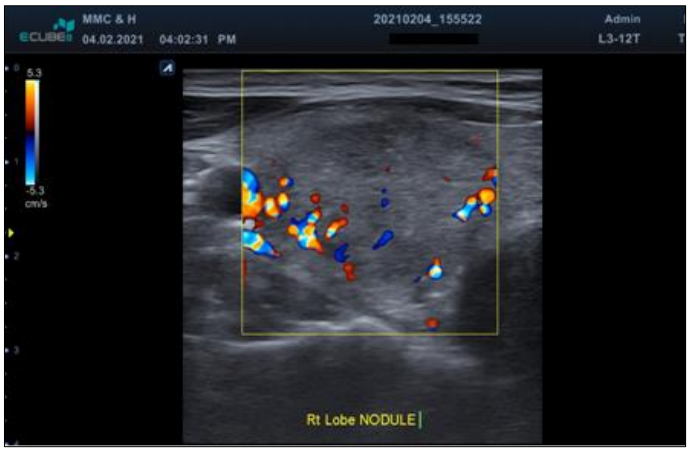

Image 2: Multinodular goiter. 46 years old male with swelling in midline of neck. On USG, B/L lobes of thyroid gland had multiple heterogeneous nodules with hypoechoic halo and peripheral vascularity.

ISSN 2515-8260 Volume 09, Issue 02, 2022

Image 3: Multinodular Goitre: Axial CECT scan showing multiple enhancing nodules in B/L lobes of thyroid gland.

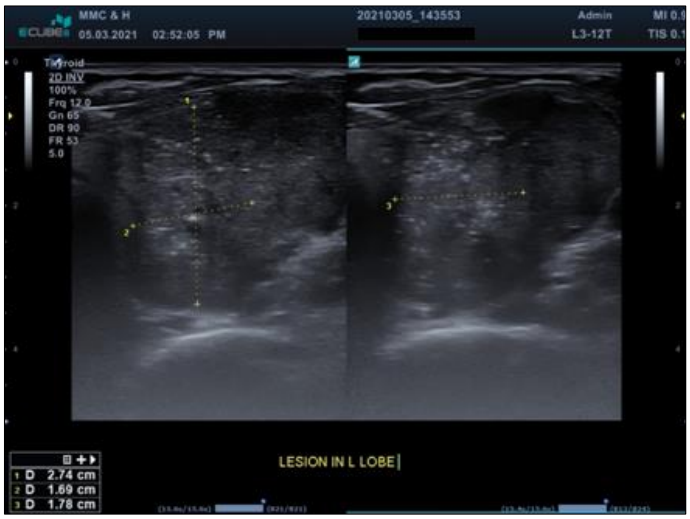

Image 4: Papillary Carcinoma Thyroid: USG showing a heterogeneous lesion with irregular margins and microcalcifications in left lobe of thyroid gland. The lesion is taller than wider and shows intense internal vascularity on color Doppler.

Image 5: Papillary Carcinoma Thyroid: USG showing a heterogeneous lesion with irregular margins and microcalcifications in left lobe of thyroid gland. The lesion is taller than wider and shows intense internal vascularity on color Doppler.

ISSN 2515-8260 Volume 09, Issue 02, 2022

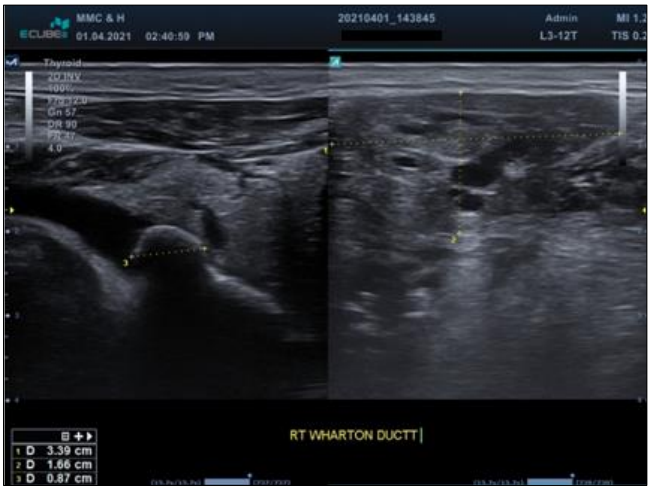

Image 6: Right submandibular sialadenitis with sialolithiasis. Right submandibular gland is heterogeneous in echotexture with multiple intraglandular ducts. The wharton's duct is dilated with calculus noted within.

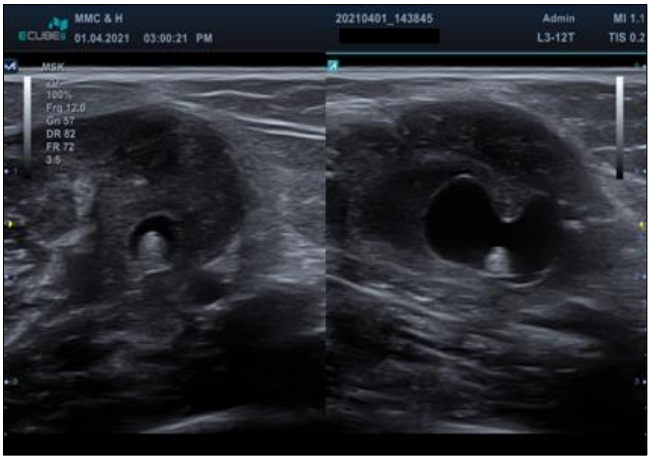

Image 7: Right submandibular sialadenitis with sialolithiasis. Right submandibular gland is heterogeneous in echotexture with multiple intraglandular ducts. The wharton's duct is dilated with calculus noted within.

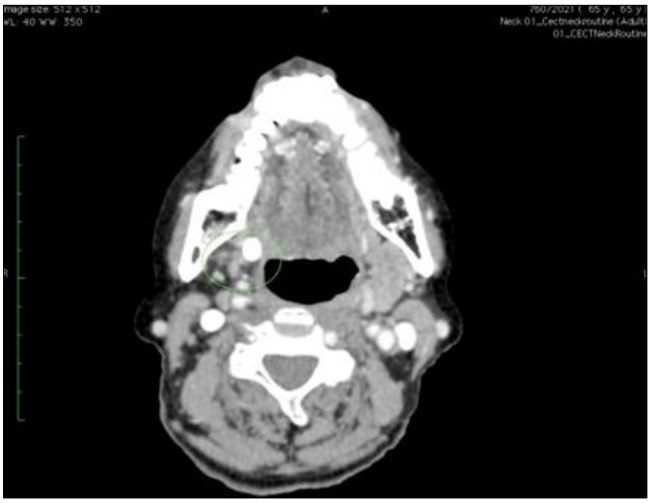

Image 8: Right submandibular sialadenitis with sialolithiasis. Axial CECT scan showing small and heterogeneous right submandibular gland with calculus noted in the wharton's duct.

ISSN 2515-8260 Volume 09, Issue 02, 2022

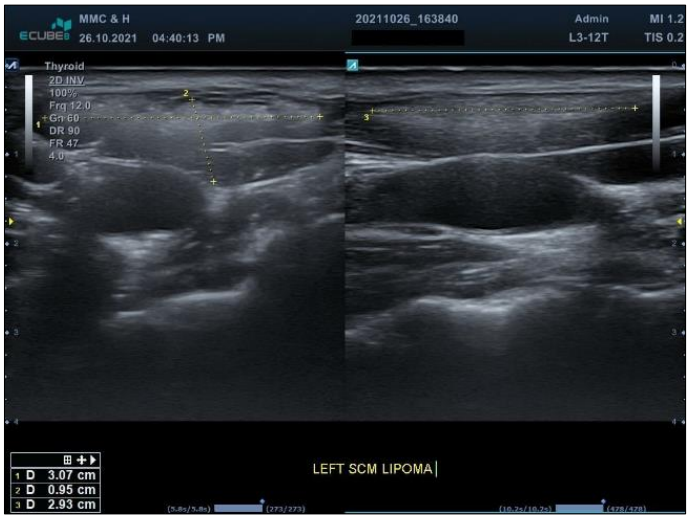

Image 9: Lipoma. 45 year old male with a well-defined hyperechoic lesion with no internal vascularity in left sternocleidomastoid muscle.

Image 10: Lipoma. Axial CT scan of the same patient showing a well circumscribed hypodense mass within the left sternocleidomastoid muscle with a dominant fat density reading -120 HU.

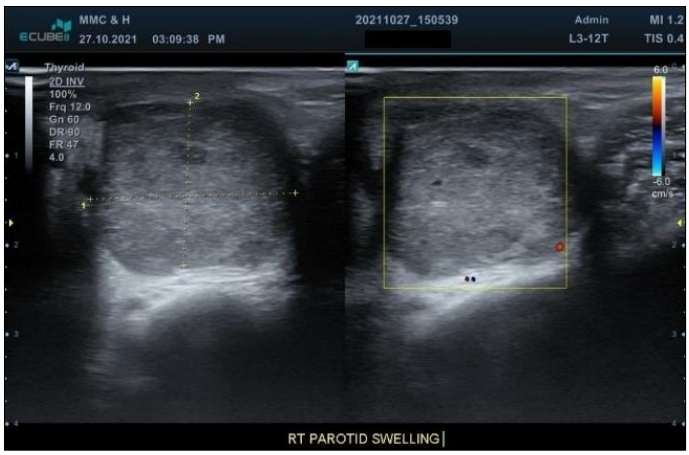

Image 11: Parotid adenoma.17 years male with swelling near right preauricular area. On USG, multilobulated heterogeneous lesion with minimal internal vascularity in right parotid gland.

ISSN 2515-8260 Volume 09, Issue 02, 2022

Image 12: Parotid adenoma. 17 years male with swelling near right preauricular area. Axial CT scan showing a large well defined heterogeneous lesion in right parotid gland.

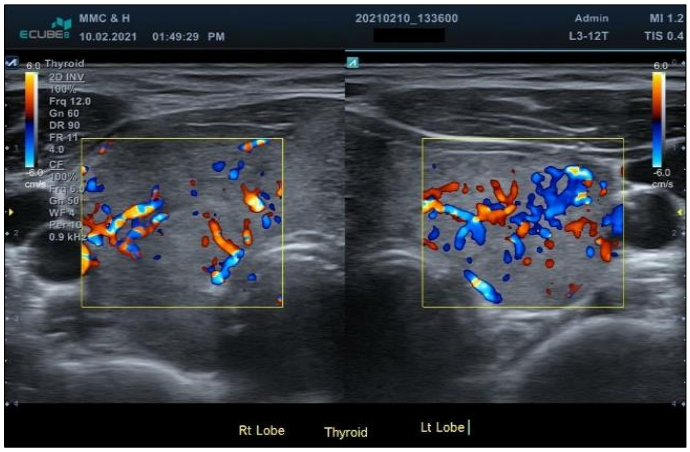

Image 13: Thyroiditis. 30 years old female with swelling in midline neck shows enlarged and heterogeneous B/L lobes of thyroid with increased internal vascularity on color Doppler.

Image 14: Metastatic lymhadenopathy. 65 years old female with biopsy proven carcinoma soft palate shows a large ill-defined lobulated mass lesion in left cervical region near common carotid artery and jugular vein. On histopathology it was confirmed to be malignant lymph nodal mass.

Image 15: Metastatic lymhadenopathy. 65 years old female with biopsy proven CA soft palate shows a large ill-defined lobulated mass lesion in left cervical region near common carotid artery and jugular vein. On histopathology it was confirmed to be malignant lymph nodal mass.

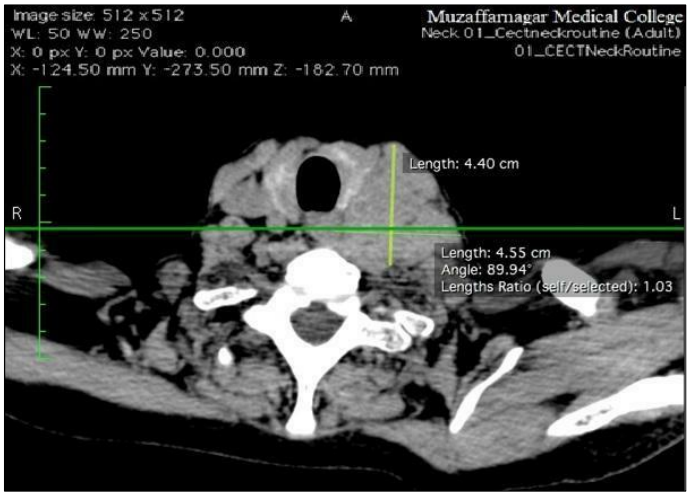

Image 16: Metastatic lymphadenopathy. Axial CECT scan of the same patient shows an ill-defined heterogeneously enhancing mass abutting left thyroid gland.

Image 17: Metastatic lymphadenopathy. Coronal CECT scan of the same patient shows the mass extending upto anterior mediastinum and encasing left common carotid and left external carotid arteries medially.

ISSN 2515-8260 Volume 09, Issue 02, 2022

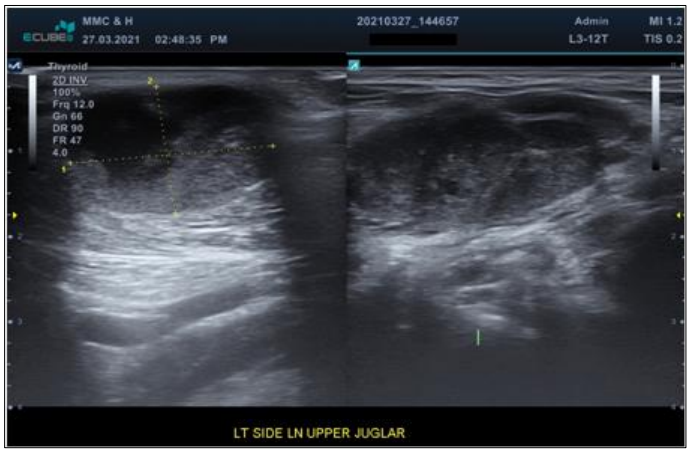

Image 18: Tubercular lymphadenopathy. Multiple enlarged matted lymph nodes with loss of central hilar fat in left upper jugular region.

Image 19: Fibromatosis colli. 1 year old child with torticollis and swelling in right cervical region shows fusiform enlargement of the right sternocleidomastoid muscle accompanied by disruption of the normal striated appearance of the muscle. Mild hyperemia is seen within the muscle, without evidence of focal mass lesion.

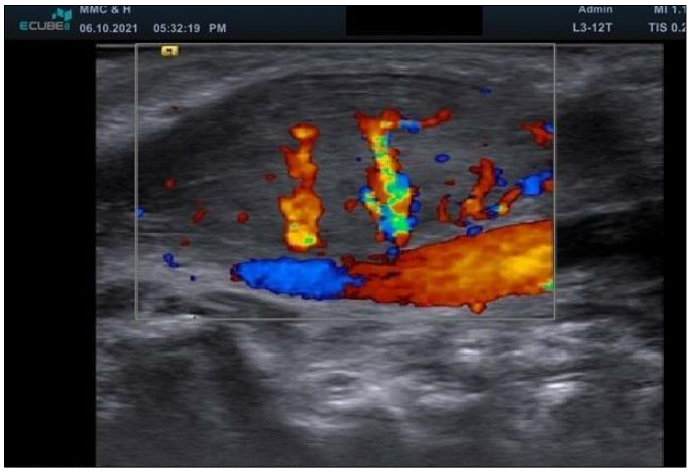

Image 20: Fibromatosis colli. 1 year old child with torticollis and swelling in right cervical region shows fusiform enlargement of the right sternocleidomastoid muscle accompanied by disruption of the normal striated appearance of the muscle. Mild hyperemia is seen within the muscle, without evidence of focal mass lesion.

ISSN 2515-8260 Volume 09, Issue 02, 2022

Conclusion

High-resolution sonography with colour doppler is an effective diagnostic tool for neck masses in people of all ages. It is a straightforward, non-invasive, and low-cost diagnostic technique. It produces precise and repeatable outcomes. It can be employed as a first-line method for evaluating cervical soft tissue masses in many clinical situations, notably in young and paediatric populations. In benign lesions, CT ensures excellent anatomical localization and lesion characterisation. It is effective for staging malignant tumours and offers crucial information about the tumour extent, which directly influences the surgical technique required for curative resection.

References

1. Bhasker N. Review of Head and Neck Masses in the Indian Population Based on Prevalence and Etiology with an Emphasis on Primary Diagnostic Modalities. Cureus, 2021, 13(7).
2. Koch BL, Hamilton BE, Hudgins PA, Harnsberger HR. Diagnostic Imaging: Head and Neck E-Book. Elsevier Health Sciences, 2016 Nov 22.
3. Wippold FJ. Head and neck imaging: the role of CT and MRI. Journal of Magnetic Resonance Imaging: Official J Int Society Magnet Resonance Med. 2007;25(3):453-65.
4. Srirangaprasad K, George GK, Pruthvi RS. Clinical Study of Preoperative Neck Masses with Computed Tomography (CT)/Magnetic Resonance Imaging (MRI) Findings and Fine Needle Aspiration Cytology (FNAC) for Appropriate Surgical Management. J Evol Med Dent Sci. 2018;7(18):2261-6.
5. Pratap V, Jain SK, Choudhary AK, Prakash O. Efficacy evaluation of ultrasonography and computerized tomography in palpable neck masses. J Evol Med Dent Sci. 2013;2(41):7891-8.
6. Wenig BM. Atlas of head and neck pathology. Elsevier Health Sciences, 2015 Aug 26.
7. Charan I, Kapoor A, Kumar N, Jagawat N, Singhal MK, Kumar HS. Evaluation of neck mass with computed tomography: an observational study. Int J Sci Stud, 2014, 2(7).
8. Becker M, Zbären P, Casselman JW, Kohler R, Dulguerov P, Becker CD. Neoplastic invasion of laryngeal cartilage: reassessment of criteria for diagnosis at CT imaging. Radiology. 2008 Nov;249(2):551-9.
9. Vaid S, Lee YY, Rawat S, Luthra A, Shah D, Ahuja AT. Tuberculosis in the head and neck a forgotten differential diagnosis. Clin Radiol. 2010;65(1):73-81.
10. Thoeny HC. Salivary glands and lymph nodes. Cancer Imaging, 2015, 15(Suppl 1).
11. Goutam AK, Kushwah AP, Pande S. Ultasonography and CT evaluation of neck masses. Int J Contemp Medi Res. 2017;4(6):1392-97.
12. Freling N, Roele E, Schaefer-Prokop C, Fokkens W. Prediction of deep neck abscesses by contrast-enhanced computerized tomography in 76 clinically suspect consecutive patients. Laryngoscope. 2009;119(9):1745-52.
13. Abd El-Monem MH, Gaafar AH, Magdy EA. Lipomas of the head and neck: presentation variability and diagnostic work-up. J Laryngol Otol. 2006;120(1):47-55.
14. Kraus J, Plzák J, Bruschini R, Renne G, Andrle J, Ansarin M, *et al*. Cystic lymphangioma of the neck in adults: a report of three cases. Wiener klinische Wochenschrift. 2008;120(7):242-5.
15. Sahu CD, Netam SB, Kumar S, Gahine R, Mungutwar V, Jaiswal A. Role of Multidetector Computed Tomography Scan in Evaluation of Neck Mass, 2018.